

FIGURE 4.1. HuR binds to the *PDCD4* transcript and modulates steady-state *PDCD4* mRNA and protein levels in MCF-7 cells. Endogenous HuR protein was immunoprecipitated from MCF-7 cells using either HuR antibody-coated protein A beads or isotype control Mouse IgG-coated beads. *A*) Proteins from the Input, unbound (UB) and Bound fractions were resolved on an SDS-PAGE gel and subjected to immunoblotting with HuR antibody. HuR was detected in the HuR bound fraction but not the IgG bound fraction. *B*) RNA isolated from the HuR RNA-IP was subjected to qRT-PCR analyses with *GAPDH*, *ER Alpha* and *PDCD4* primers. mRNA levels in HuR bound fractions were normalized to input levels and then compared by fold-enrichment over IgG control. Significant enrichment of *ER α* and *PDCD4* transcripts was observed with HuR IP. *C*) MCF-7 cells transiently transfected with Scramble or HuR siRNA (siScr. and siHuR, respectively) were subjected to immunoblot analysis with HSP90, HuR, or *PDCD4* antibody. Steady-state *PDCD4* protein levels were normalized to HSP90 loading control and siScramble set to 1.00. A decrease in *PDCD4* steady-state protein levels upon HuR knockdown is quantified below the representative blot. *D*) qRT-PCR analysis of total RNA isolated from siRNA-treated cells with *PDCD4* and *RPLP0* primers demonstrates a significant decrease in *PDCD4* steady-state mRNA levels upon HuR knockdown. Values represent the mean \pm SEM for n=3 independent experiments. ** represents $p \leq 0.01$.

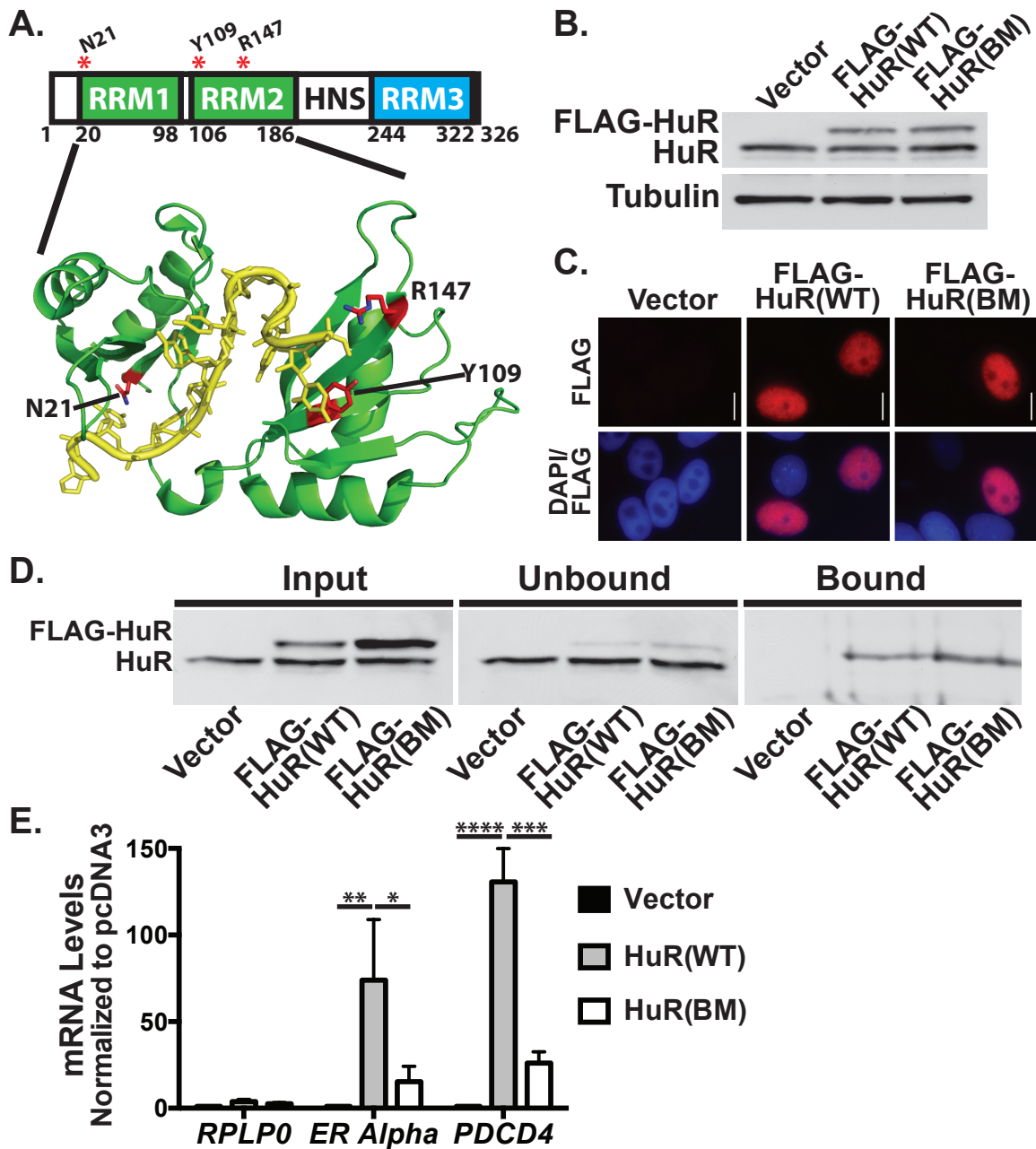


FIGURE 4.2. Key residues in HuR RRM1 and 2 are required for binding to ARE-containing target mRNAs, including *PDCD4*. A) The HuR protein contains three RRM1, RRM2 and RRM3) and a HuR Nucleocytoplasmic Shuttling sequence (HNS), which mediates bidirectional transport of HuR between the nucleus and cytoplasm (16). The two N-terminal RRMs (green) are responsible for ARE recognition while the C-terminal RRM (blue) is thought to bind to the poly(A) tail of mRNA transcripts. Shown below the linearized map of HuR is a recently solved co-crystal structure (PDB # 4ED5) of HuR RRM1 and RRM2 (green) in complex with an AUUUUUUAUUUU RNA oligomer (yellow). Residues shown to be important for RNA recognition in *in vitro* binding studies are highlighted in red (N21, Y109 and R147). A putative HuR RNA binding mutant (BM) was generated by changing these residues to alanine in a FLAG-

tagged HuR expression construct. *B*) MCF-7 cells were transfected with vector control, FLAG-HuR(WT) or -HuR(BM) plasmids and subjected to immunoblotting with HuR and Tubulin antibodies. FLAG-HuR proteins were detected only in FLAG-transfected cells and levels of BM are comparable to WT. *C*) Transfected MCF-7 cells were analyzed by indirect immunofluorescence with FLAG antibody to detect FLAG-HuR(WT) or (BM). Colocalization with DAPI reveals steady-state nuclear localization of both FLAG-HuR proteins (WT and BM). Scale bar, 10 μ m. *D*) Cells expressing vector control or FLAG-HuR proteins were subjected to RNA-IP using FLAG antibody-conjugated beads. Immunoblot analysis of IP samples demonstrates specific enrichment of FLAG-HuR proteins in bound fractions. *E*) RNA that co-precipitated with FLAG-HuR proteins was subjected to qRT-PCR analyses with *RPLP0*, *ER Alpha* and *PDCD4* primers to detect bound transcripts. *ER Alpha* and *PDCD4* transcripts were significantly enriched upon wildtype HuR purification; however, a significant decrease in enrichment was observed upon purification of HuR binding mutant. mRNA levels in FLAG-HuR-bound fractions were normalized to input levels and then compared by fold-enrichment over vector control samples. Values represent the mean \pm SEM for n=3. *, **, *** and **** represents $p \leq 0.05$, $p \leq 0.01$, $p \leq 0.001$ and $p \leq 0.0001$, respectively.

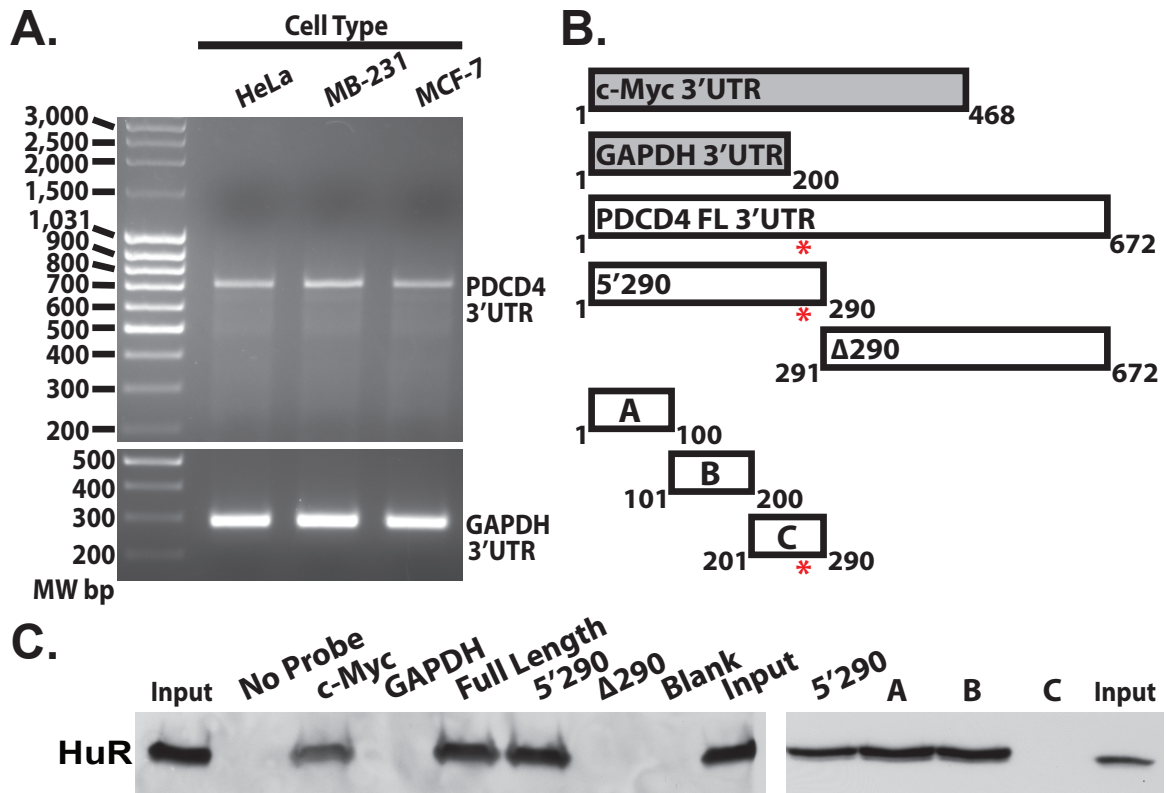


FIGURE 4.3. HuR binds to sites within the *PDCD4* 3'UTR. *A*) Total RNA isolated from HeLa, MB-231 and MCF-7 cells was subjected to 3'RACE analysis using *PDCD4* and *GAPDH* 3'UTR-specific primers as described in Materials and Methods. PCR products were resolved on a 2% agarose gel and represent the 3'UTR plus the length of the primers used for amplification. The *PDCD4* 3'UTR is 672 nt and was verified by sequencing. The *GAPDH* 3'UTR is shown as a control. Molecular weight markers in base pairs (MW bp) are shown to the left of the gel. *B*) Biotinylated probes corresponding to the 3'UTRs of the *c-Myc*, *GAPDH* and *PDCD4* transcripts were generated and used for biotin pulldown experiments in MCF-7 cells. The red asterisk denotes the well-defined *miR-21* seed region (46) in the *PDCD4* 3'UTR. The *PDCD4* 3'UTR was also dissected to generate various biotin probes that represent different regions of the transcript. *C*) Proteins that co-precipitated with the avidin-bound biotinylated probes, as shown in (*B*), were subjected to immunoblotting with HuR antibody. HuR protein co-precipitates with a probe corresponding to the *c-Myc* 3'UTR as well as the first two 100 nt regions of the *PDCD4* 3'UTR. Images are representative of n=3 independent experiments.

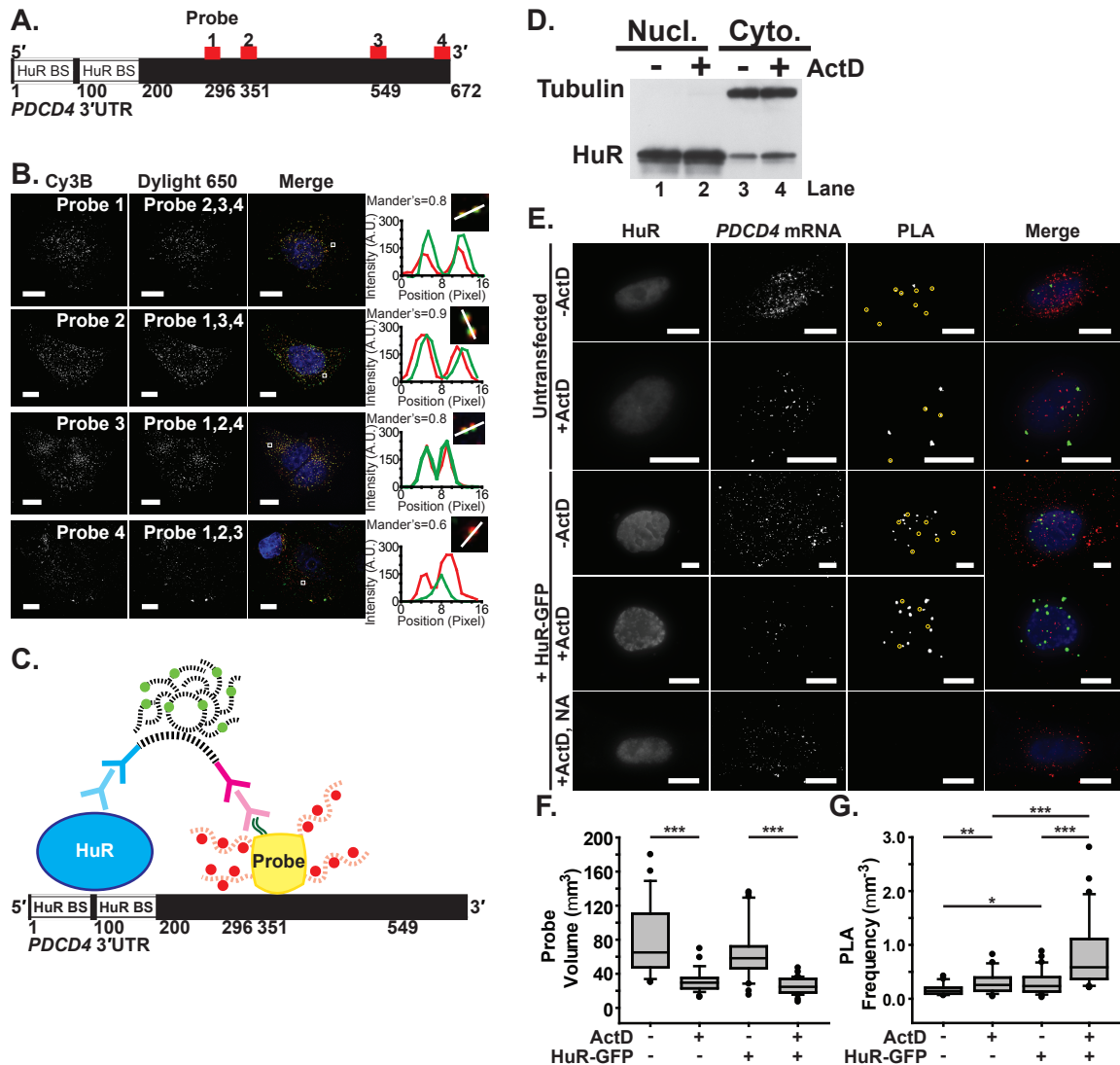


FIGURE 4.4. Visualization of HuR-*PDCD4* interactions in situ using FLAG-tagged probes. *A*) The 672 nt *PDCD4* 3'UTR contains two HuR binding sites (HuR BS) within the first 200 nt. Four mRNA probes (1, 2, 3 and 4) were designed to target distinct positions within the *PDCD4* 3'UTR (shown in red). *B*) Each of four *PDCD4* 3'UTR probes labeled with Cy3B fluorophores was delivered to MCF-7 cells along with the other three probes labeled with Dylight 650 fluorophores. Merge images of Cy3B-labeled probe (red), Dylight 650-labeled probe (green), and DAPI-stained nuclei (blue) are also shown. All image planes are represented. Magnified, merge images of overlapping probes in the boxed region are shown with profile plot of the fluorescence intensity of Cy3B (red) and Dylight 650 (green) along an intersection of the probes (white line). Scale bar, 10 μ m. The mean Mander's coefficient of Cy3B and Dylight 650 probe colocalization is shown. *C*) A schematic of the proximity ligation assay (PLA), which measures the interaction between HuR and probes specific to the *PDCD4* 3'UTR is shown. As described in Experimental Procedures, PLA was performed between HuR and FLAG-tagged (dark green lines) probes with four Cy3b-labeled (red) oligonucleotides (red dash lines) and a neutravidin core (yellow) in nucleotides 296-549 of the *PDCD4*

3'UTR. Anti-HuR mouse primary antibody (light blue) and anti-mouse PLA probe (dark blue) bind to HuR, while anti-FLAG rabbit primary antibody (light magenta) and anti-rabbit PLA probe (dark magenta) bind to FLAG. Once they are in proximity, the oligonucleotides (black dash lines) attached to the PLA probe come together via ligation to form a template for DNA polymerase, which resulted in a coiled DNA product that can be labeled with Cy5-equivalent fluorophore (light green) bound complementary DNA strands (black dash lines). *D*) MCF-7 cells treated with vehicle control or Actinomycin D (ActD) for 90 minutes were subjected to subcellular fractionation (as described in Experimental Procedures) and subsequent immunoblotting with HuR and Tubulin antibody. A distinct enrichment of HuR is observed in the cytoplasm upon ActD treatment. *E*) HuR, *PDCD4* mRNA and PLA between HuR and *PDCD4* mRNA were imaged in untransfected and HuR-GFP transfected MCF-7 cells exposed to (+ActD) or unexposed to (-ActD) actinomycin D. MCF-7 cells transfected with HuR-GFP and exposed to ActD received *PDCD4* mRNA probes with neutravidin lacking the FLAG tag (NA) and were used as a negative control. PLA punctae that are less than 2 μ m in diameter have been marked with yellow circles. Merge images of HuR (blue), *PDCD4* mRNA (red) and PLA between HuR and *PDCD4* mRNA (green) are shown. All image planes are represented. Scale bar, 10 μ m. *F*) Probe volume (μ m³) measured for each untransfected and HuR-GFP transfected cell exposed or unexposed to ActD (Untransfected: n=46 cells; Untransfected, +ActD: n=125; HuR-GFP transfected: n=51; HuR-GFP transfected, +ActD: n=62). *G*) PLA frequency normalized to the probe volume (μ m⁻³) for each cell. * represents $p \geq 0.025$, $p < 0.05$; ** represents $p > 0.001$, $p < 0.025$; *** represents $p < 0.001$ (one-way ANOVA with Dunn's method).

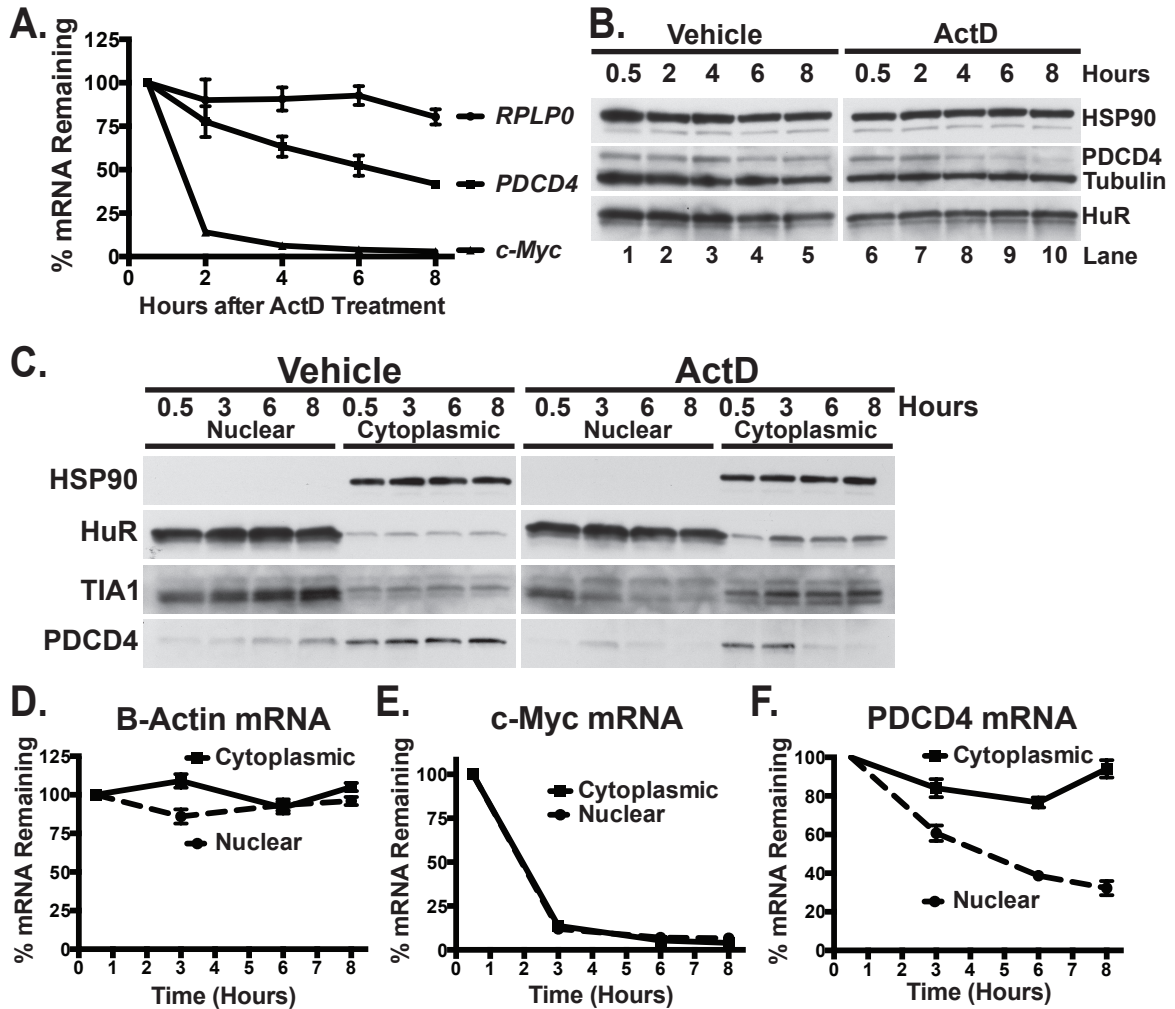


FIGURE 4.5. The cytoplasmic pool of *PDCD4* mRNA is highly stable compared to the nuclear pool. *A)* MCF-7 cells were treated with ActD and collected at the indicated time points after drug addition. Total RNA isolated from ActD-treated cells was subjected to qRT-PCR analysis with *RPLP0*, *PDCD4* and *c-Myc* primers. mRNA levels are represented as % of amount present at 30 minutes of ActD exposure. The half-life of the *c-Myc* and *PDCD4* transcripts was calculated to be 1.6 and 6.1 hours, respectively. *B)* Immunoblot analysis of total protein isolated from the samples in (*A*) to detect *PDCD4*, *HSP90*, *Tubulin* and *HuR* reveal a sharp decrease in *PDCD4* protein upon treatment with ActD, but not vehicle control. *C)* MCF-7 cells treated with vehicle control or ActD over the indicated time course were subjected to subcellular fractionation followed by immunoblotting with *HSP90*, *HuR*, *TIA1*, or *PDCD4* antibody. Immunoblots reveal an accumulation of both *HuR* and *TIA1* in the cytoplasm across the ActD time course, but no accumulation is observed during vehicle control treatment, as expected. *PDCD4* is predominantly cytoplasmic in these cells and the cytoplasmic pool of *PDCD4* demonstrates the robust decrease after ~3 hours of ActD treatment. RNA isolated from nuclear and cytoplasmic fractions from (*C*) were subjected to qRT-PCR analysis with β -actin (*D*), *c-Myc* (*E*) and *PDCD4* (*F*) primers. The decay profiles of β -actin and *c-Myc* mRNA are similar between the nuclear and cytoplasmic compartments (*D* and *E*), however the cytoplasmic pool of

PDCD4 mRNA displays a significantly increased decay profile compared to the nuclear pool of *PDCD4* mRNA (*F*). Ct values were normalized to *18s rRNA* and decay profiles are represented as % of amount at 30 minutes of ActD exposure. Data points represent the mean \pm SEM for n=3 independent experiments. * represents p<0.05. Images are representative of n=3 independent experiments.

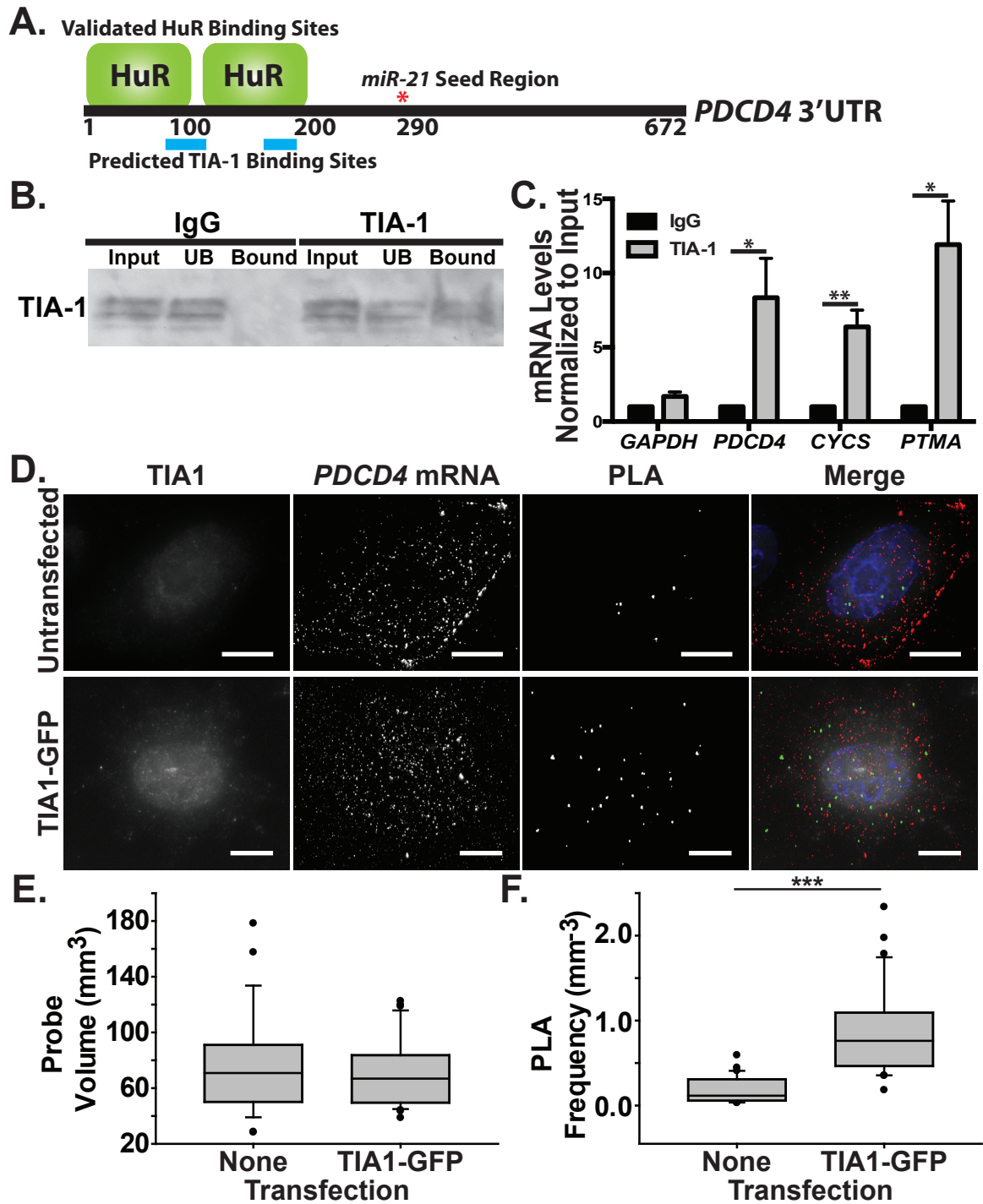


FIGURE 4.6. The RNA binding protein, TIA1, interacts with *PDCD4* mRNA. *A*) A recent TIA1 iCLIP study reveals two predicted TIA1 binding sites (shown here in blue) within the first 200 nt of the *PDCD4* 3'UTR (27) that overlap with the validated HuR binding sites (green) defined here. The red asterisk denotes the well-defined *miR-21* seed region. *B*) Endogenous TIA1 protein was immunoprecipitated from MCF-7 cells using TIA1 antibody-coated protein A beads alongside isotype control Goat IgG-coated beads.

Proteins from the Input, unbound (UB) and Bound fractions were subjected to immunoblotting with TIA1 antibody. TIA1 was detected in the TIA1-bound fraction but not the control IgG bound fraction. TIA1 is alternatively spliced to generate two distinct protein products that correspond to the two bands detected. *C*) qRT-PCR analysis of RNA isolated from the TIA1 RNA-IP using *PDCD4*, *CYCS* and *PTMA* primers reveals clear enrichment of these transcripts upon TIA1 pulldown. A control mRNA, *GAPDH*, did not co-precipitate with TIA1. Values represent the mean \pm SEM for n=3 independent experiments. * and ** represent $p \leq 0.05$ and $p \leq 0.01$, respectively. *D*) PLAs performed with TIA1 antibody and *PDCD4* 3'UTR probes 1-3 reveal interactions between TIA1 and the *PDCD4* 3'UTR. Merge images of nuclei (blue), TIA1 (white), *PDCD4* mRNA (red) and PLA between TIA1 and *PDCD4* mRNA (green) are shown. All image planes are represented. Scale bar, 10 μm . *E*) Probe volume (μm^3) measured for each untransfected (n=11 cells) and TIA1-GFP transfected (n=15) cell. *F*) The PLA frequency normalized to the probe volume (μm^3) for each cell. *** represents $p < 0.001$ (Mann-Whitney rank sum test).

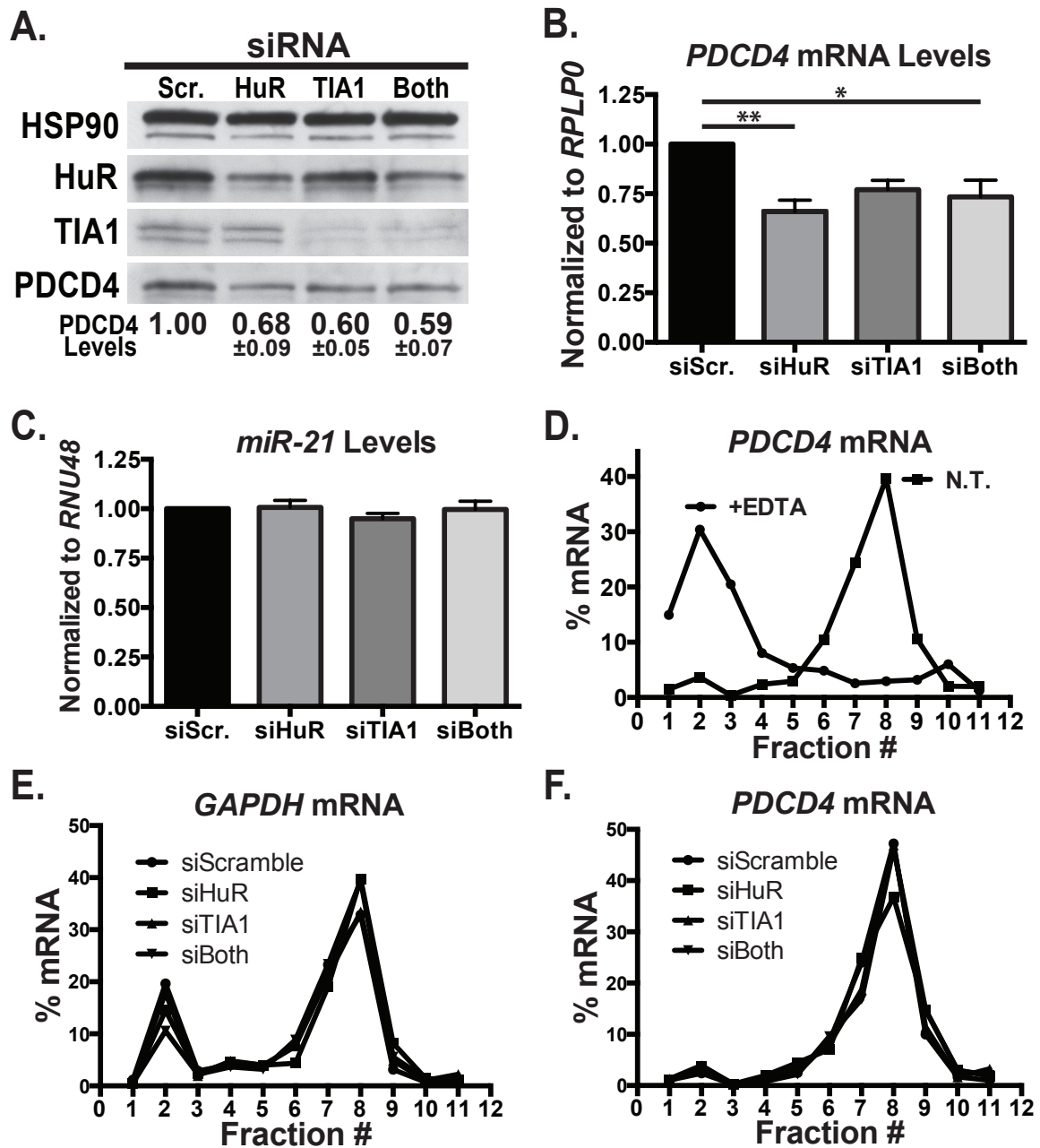


FIGURE 4.7. Knockdown of HuR and TIA1 lead to decreased *PDCD4* steady-state mRNA and protein levels. *A)* MCF-7 cells transiently transfected with Scramble, HuR and/or TIA1 siRNA (siScr., siHuR, siTIA1 and siBoth) were subjected to immunoblot analysis with HSP90, HuR, TIA1 or PDCD4 antibody. Steady-state PDCD4 protein levels were normalized to HSP90 loading control and siScramble set to 1.00. Decreased PDCD4 steady-state protein levels upon HuR and/or TIA1 knockdown is quantified below the representative blot. *B)* qRT-PCR analysis of total RNA isolated from siRNA-treated cells with *PDCD4* and *RPLP0* primers demonstrates a significant decrease in *PDCD4* steady-state mRNA levels upon HuR and/or TIA1 knockdown. *C)* qRT-PCR analysis of steady-state *miR-21* and *RNU48* (loading control) levels upon knockdown of

HuR and/or TIA1 reveals no significant difference in *miR-21* levels across all treatment groups. D) Polysome profiling was performed on MCF-7 cells as described in Experimental Methods. Cytoplasmic lysates from MCF-7 cells were treated with EDTA (to disrupt polyribosomes) or left untreated (No Treatment, N.T.) and subjected to polysome fractionation. Untreated MCF-7 cells demonstrate active translation of *PDCD4* mRNA (as represented by a sharp peak in fraction 8) while EDTA-treated cell lysates display a collapse of the polyribosomes on the *PDCD4* transcript, as expected. Polysome profiling was performed on MCF-7 cell lysates transfected with scramble control, HuR and/or TIA1 siRNA. Analysis of the *GAPDH* (E) and *PDCD4* (F) transcripts reveals that *PDCD4* mRNA is actively translated in MCF-7 cells, similar to *GAPDH*, and that knock-down of HuR and/or TIA1 has no effect on the translation of the *PDCD4* transcript under these conditions. Polysome profiles are representative of two technical qRT-PCR replicates of a single fractionation experiment. Values represent the mean \pm SEM for n=3 independent experiments. * and ** represents $p \leq 0.05$ and $p \leq 0.01$, respectively.

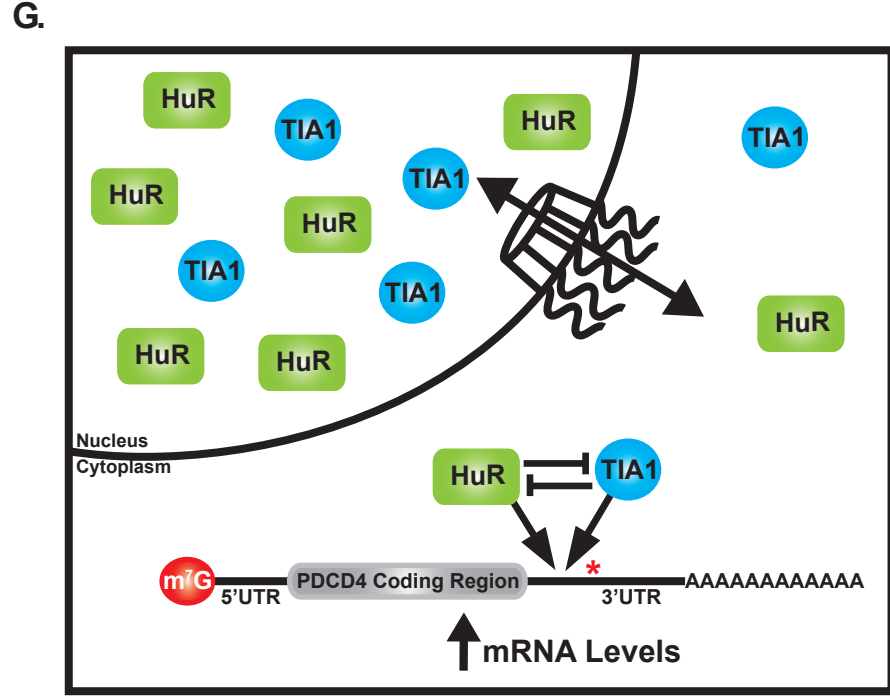
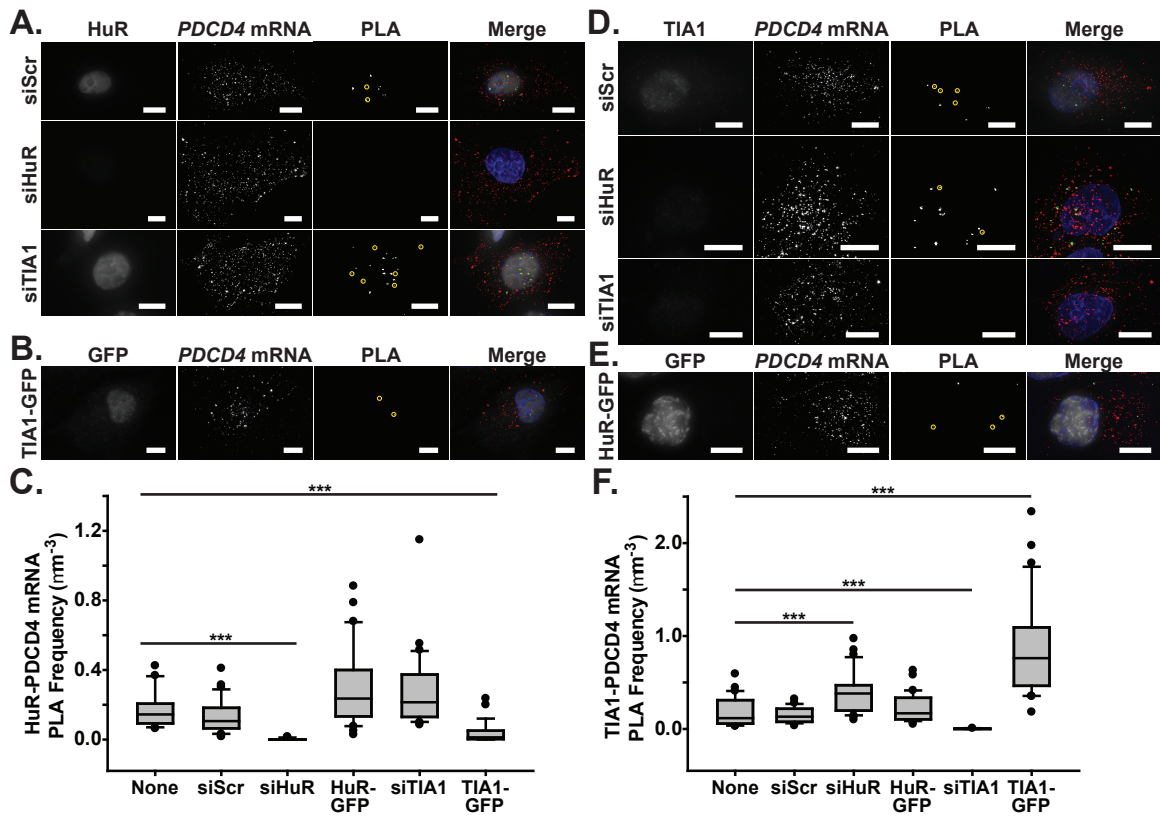


FIGURE 4.8. HuR and TIA1 compete for binding to the *PDCD4* 3'UTR. *A)* Visualization of HuR protein, *PDCD4* mRNA and interaction between HuR and *PDCD4* mRNA (PLA) in control cells transfected with scrambled siRNA (siScr), or siRNA directed against either HuR (siHuR) or TIA1 (siTIA1). Merged images of HuR (white), *PDCD4* mRNA (red), PLA (green) and nuclei (blue) are also shown. PLA punctae that are less than 2 μ m in diameter have been marked with yellow circles. All image planes are represented. Scale bar, 10 μ m. *B)* Visualization of GFP, *PDCD4* mRNA and interaction between HuR and *PDCD4* mRNA in TIA1-GFP transfected cells. Merged images of GFP (white), *PDCD4* mRNA (red), PLA (green) and nuclei (blue) are also shown. PLA punctae that are less than 2 μ m in diameter have been marked with yellow circles. All image planes are represented. Scale bar, 10 μ m. *C)* HuR-*PDCD4* mRNA PLA frequency normalized to probe volume (μ m³) for untransfected (n=46 cells), siScramble (n=81), siHuR (n=25), HuR-GFP (n=51), siTIA1 (n=97), and TIA1-GFP (n=69) cells. *** represents p<0.001 (one-way ANOVA with Dunn's method). *D)* Visualization of TIA1 protein, *PDCD4* mRNA and PLA interaction between TIA1 and *PDCD4* mRNA in siScramble (siScr), siHuR and siTIA1 transfected cells. Merged images of TIA1 (white), *PDCD4* mRNA (red), PLA (green) and nuclei (blue) are also shown. PLA punctae that are less than 2 μ m in diameter have been marked with yellow circles. All image planes are represented. Scale bar, 10 μ m. *E)* Visualization of GFP, *PDCD4* mRNA and PLA interaction between TIA1 and *PDCD4* mRNA in HuR-GFP transfected cells. Merged images of HuR (white), *PDCD4* mRNA (red), PLA (green) and nuclei (blue) are shown. PLA punctae that are less than 2 μ m in diameter have been marked with yellow circles. All image planes are represented. Scale bar, 10 μ m. *F)* TIA1-*PDCD4* mRNA PLA frequency normalized to probe volume (μ m³) for untransfected (n=55 cells), siScramble (n=49), siHuR (n=66), HuR-GFP (n=46), siTIA1 (n=44), and TIA1-GFP (n=76) cells. *** represents p<0.001 (one-way ANOVA with Dunn's method). *G)* Model for the post-transcriptional regulation of *PDCD4* mRNA in the cytoplasm. In MCF-7 cells, the steady-state localization of both HuR (green rectangle) and TIA1 (blue circle) is predominantly nuclear with a small pool that shuttles in and out of the cytoplasm (black bi-directional arrow). We observe a competitive mode of binding between HuR and TIA1 on the *PDCD4* 3'UTR in the cytoplasm, in close proximity to a well-defined *miR-21* binding site (red asterisk).